ORIGINAL RESEARCH (AR) DOI: 10.4274/jems.2024.44711

Journal of ETA Maritime Science 2024;12(3):237-251

Modeling Investigation of Potential Sea Level Rise Effect on Hydrodynamics and Sediment Transport in Hyères Bay, France

Minh Tuan Vu[1], Yves Lacroix[2], Viet Thanh Nguyen[3]

[1]Institute of Port and Maritime Techniques, Hanoi University of Civil Engineering, Hanoi, Vietnam
[2]SeaTech, University of Toulon, Toulon, France
[3]Department of Civil Engineering, University of Transport and Communications, Hanoi, Vietnam

Abstract

Global climate change increases storm frequency and Sea Level Rise (SLR). This leads to an increased risk of coastal flooding, reduced effectiveness of protective structures, and intensified coastal erosion and retreat. The Bona and Ceinturon beaches, two beautiful sandy beaches with low-lying topography along the eastern branch of the Giens double tombolo on the western coast of Hyères Bay, have high tourist value. These areas are very vulnerable to SLR, which is believed to reduce the effectiveness of the shore protection structures built on these sandy beaches. The effects of SLR on changes in the hydrodynamic characteristics of these water bodies need to be quantified. This may help clarify the relationship between SLR and coastal erosion. This study investigated the variation of wave height and current speed due to SLR at the Bona and Ceinturon beaches using a coupled numerical model. The performance of this model was calibrated by comparing the model results with the in situ measured data. The research results are the basis for assessing the impact of SLR due to climate change on this area and provide a useful solution for coastal management in the future.

Keywords: Giens tombolo, SLR, Numerical model, Hydrodynamic, Sediment transport rate

1. Introduction

According to the report of IPCC [1], the melting of glaciers and ice sheets in the polar regions and in the high mountains and the global spatial expansion due to climate change are the main causes of global sea level rise. However, within the Mediterranean Sea, a semi-enclosed basin, atmospheric forcing changes, and ocean circulation mainly cause the sea level to rise. This sea has been experiencing sea level rise differently from the global mean [2]. The mean sea level in the Mediterranean Sea increased at a rate (1.1-1.3 mm/year) lower than the global mean sea level (1.8±0.5 mm/year) during the 20th century [3]. Through satellite altimetry, Cazenave et al. [4] found that the mean sea level in the area from Marseille to Menton increased at a rate of approximately +2.2 mm/year during 1993-2013. In the 21st century, Galassi and Spada [5] predicted that future sea level changes in the Mediterranean Sea in 2040-2050 compared with 1990-2000 would be 9.8 cm in the minimum scenario and 25.6 cm in the maximum scenario. Specifically, a sea level rise rate of about 1.26±0.05 mm/year is estimated by a linear regression method based on sea level data measured at Marseille station in the period of 1885-2012. On the other hand, the sea level of Marseille station in 2040-2050 is forecasted to rise by about +1.2 mm/year in the minimum scenario and +4.2 mm/year in the maximum scenario.

The coastal areas are home to more than 50% of the world's population. However, these regions could suffer severe impacts if the global sea level rises by approximately 44 cm by 2100 [6]. Sea level rise typically entails many severe risks to coastal areas, including increased volume of sediment lost along the coast and offshore, flooding or submergence of coastal marshes and lowlands, increasing saltwater intrusion into estuaries, rivers, and aquifers, exacerbating the problem of environmental pollution in urban areas as well as damage from storms and floods [7], and displacing existing coastal animal communities and plants, significantly degrading

Address for Correspondence: Minh Tuan Vu, Institute of Port and Maritime Techniques, Hanoi University of Civil Engineering, Hanoi, Vietnam
E-mail: tuanvm@huce.edu.vn
ORCID ID: orcid.org/0000-0002-6099-0603

Received: 20.11.2023
Last Revision Received: 01.06.2024
Accepted: 03.06.2024

To cite this article: M. T. Vu, Y. Lacroix, and V. T. Nguyen. "Modeling Investigation of Potential Sea Level Rise Effect on Hydrodynamics and Sediment Transport in Hyères Bay, France." *Journal of ETA Maritime Science*, [Epub Ahead of Print]

the meadows of Posidonia oceanica [8]. Furthermore, the protective effectiveness of existing coastal structures such as breakwaters, groynes, seawalls, and sea dikes could be reduced by wave overtopping or submergence due to SLR [9]. In the study area, SLR may not only have as significant an impact on the lives of local communities as in other densely populated coastal cities in the world, but it can also be vulnerable to the tourism industry. The tourism industry in this coastal region has an annual turnover of approximately 4.6 billion euros and contributes to one-fifth of the total sales of the French tourism industry [10]. Therefore, the decline or disappearance of the beaches here induced by SLR would have a substantial negative impact on the economy of this area.

Among the negative impacts of SLR, coastal erosion is a global and topical problem. Brunel and Sabatier [10] conducted a survey of the beaches of Hyères Bay. These are pocket-beaches bounded by cliffs or scarps above the backshore. It was concluded that these beaches lost an average of 40% (±10%) of their surface area due to coastal erosion, which equates to an average retreat of approximately 12.1 (±3.5) m from 1896 to 1998. The average shoreline retreat of 5.8 (±3.5) m was caused by a relative SLR of +11 cm during this period. In addition, Brunel and Sabatier [10] predicted that nearly a quarter of the surveyed pocket-beaches would likely lose at least 75% (±10%) of their present surface area with an average retreat of -20 (±2) m if SLR is increased to +44 cm due to global climate change by 2100. Using the integration of satellite remote sensing and GIS techniques, Tuan et al. [11] showed that the Bona and Ceinturon beaches were most severely eroded, with maximum erosion rates of 0.44 and 0.77 m/yr, respectively. Moreover, they predicted that the trend of shoreline retreat would continue to occur at these beaches until 2050.

The trend of global warming, along with SLR, is hard to reverse, and global climate change will not be under control in the near future. Hence, it is essential to focus more on investigating the adverse consequences of climate change. In the present study, the authors focus on simulating the changes in the hydrodynamic field around the Ceinturon beach in the eastern branch of the Giens double tombolo, considering the SLR.

2. Study Area

The Giens double tombolo is situated in the small town of Hyères city, the southernmost point of France on the Mediterranean Sea (Figure 1). The phenomenon of wave refraction and diffraction on the island of Giens is attributed to the main cause of this tombolo formation [12,13]. It consists of two sand spits separated by a salt marsh in the middle. The eastern sand spit of the Giens double tombolo

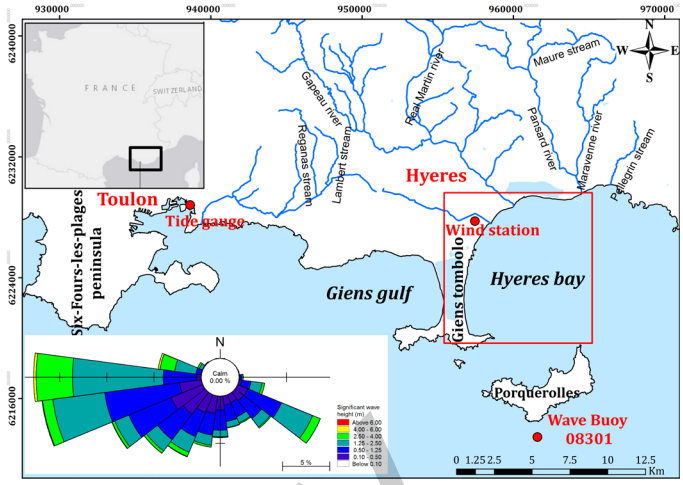

Figure 1. *Wave rose and the location of the study area*

facing Hyères Bay is bounded by the mouth of the Gapeau River to the north and the Cape of Esterel to the south. However, this sand spit is being eroded due to both natural causes and human impacts, especially Bona and Ceinturon beaches [14].

Field wind data were collected from Hyères station from 1999 to 2018. There are three main wind directions that generate waves approaching the beaches along the eastern branch of the Giens tombolo: northeast, east, and southeast morphological winds. They account for more than 28% of the total uptime. The east wind, with a frequency of 10.58%, has the highest speed of 20.31 m/s. Natural factors have the greatest influence on morphological changes in the study area [15].

Offshore wave data measured by buoy 08301 at a depth of 90 m south of Porquerolles Island (Figure 1) revealed that the waves come from three main directions. The most frequent direction is the west waves with about 36.92% of the total regime. Nevertheless, these waves do not affect the study area much and are quite difficult to penetrate into Hyères bay, as most of them are reflected or changed in the direction by the Six-Fours-les-Plages peninsula before approaching the Gulf of Giens. The second most frequent direction is west-southwest with a frequency of 28.84%. Similar to western waves, these waves are very difficult to penetrate into the study area because it is shielded by the Giens tombolo. The third dominant wave direction is east-southeast with a frequency of 19.1% of the total regime. They can spread into the study area and influence the shoreline evolution of the beaches along the eastern Giens tombolo. Wave is also the main factor affecting the hydrodynamic process in the study area because tidal fluctuations are negligible [16].

The Gapeau River, located 6 km north of the Giens tombolo, is the main source of sediment for the formation of the Giens tombolo and Hyères Bay [17] (Figure 1).

Measured discharge data were collected at the Sainte Eulalie station located approximately 6 km upstream from the mouth of the Gapeau River. The annual discharge of the Gapeau river is approximately 4 m^3/s and that of the dry season is approximately 0.5 m^3/s. Furthermore, the discharges of the decadal, tri-decadal, semi-centennial, and centennial floods are forecasted approximately 180 m^3/s, 220 m^3/s, 300 m^3/s, and 600 m^3/s, respectively [18,19].

Most of the seabed in Hyères Bay is covered with sand from organic production and Posidonia seagrass, a well-known endemic plant of the Mediterranean Sea. Sand is concentrated mainly in coastal areas. The grain size of the sand is distributed depending on the longshore current and tends to decrease from north to south. Specifically, coarse sand with a diameter of 0.55 mm occurs on the northern beaches of the study area, whereas fine sand with a diameter of 0.2 mm is observed on the southern beaches of the study area [18]. Meanwhile, Posidonia seagrass has taken over the remains of the seabed. It plays a crucial role in the hydrodynamic process and sediment transport in Hyeres Bay in general and Giens tombolo in particular [20]. Posidonia appears at very close distances from the coast. It ranges from a depth of 0 to a water depth of 30 m, covering 9200 ha in the bay of Hyères, from the south of the Giens tombolo up to Bormes-les-Mimosas [21].

3. Materials and Methods

3.1. Field Measurements

The process model calibration and validation were carried out using the in situ measurement data at La Capte beach supported by Meulé [22] and E.O.L [23]. These data are summarized here.

a. Bathymetry

Differential Global Positioning System technology has been applied to survey the bathymetry along the western and eastern parts of the double Giens tombolo from 2000 to 2010. The survey range extends approximately 500 m from the shoreline to the sea. The EOL bathymetry has zero elevation as the Lowest Astronomical Tide and uses the Nouvelle triangulation de la France horizontal coordinate reference system with the projection in Lambert III (France Sud) [23]. The bathymetry of the study area is shown in Figure 2.

b. Hydrodynamics

To obtain data on waves and currents, a measurement campaign was carried out in March 2009 by Meulé [22], where five stations with measuring devices were immersed. The five stations from SCAPT1 to SCAPT5 were installed perpendicular to the coast on a single line to understand the cross-shore hydrodynamics. They cross the geotubes furthest out to sea, and the Posidonia seagrass meadow. In total, there were four turbidity probes (OBS), four acoustic Doppler velocimeters, an acoustic Doppler current profiler (ADCP 600Khz RDI), and an electromagnetic current meter (S4DW) fixed on the five submerged stations illustrated in Figure 3.

Five stations had different measurement periods and were at different depths. Therefore, the SCAPT2 station was located at a depth of 3 m, SCAPT3 at a depth of 1.8 m, and SCAPT5 (5-1 and 5-2) was located at 1.6 m depth. On the other hand,

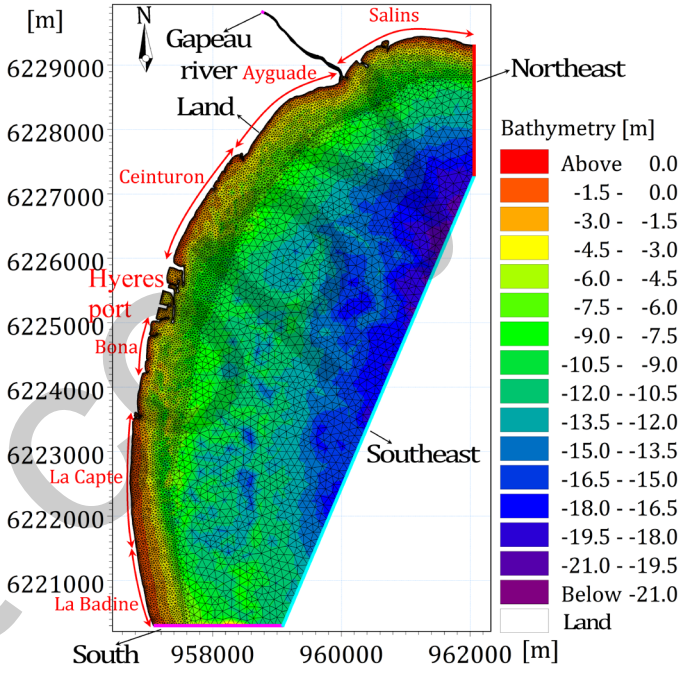

Figure 2. *Computational domain and bathymetry*

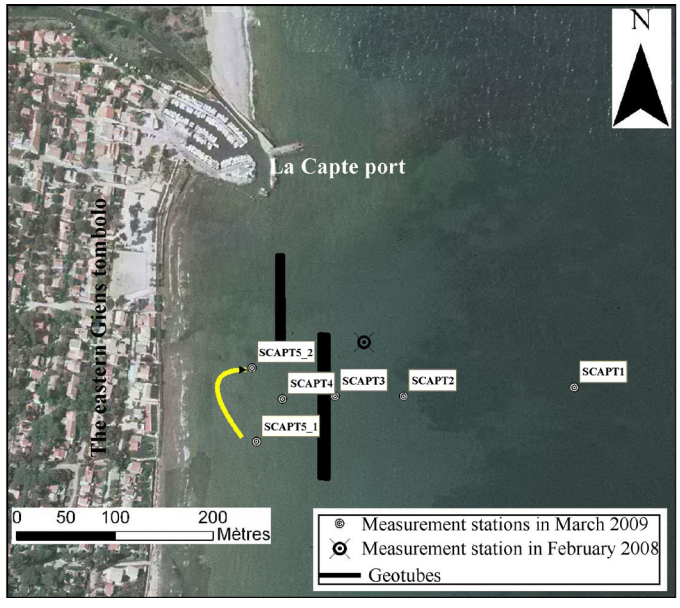

Figure 3. *Location of wave measuring stations in La Capte beach [22]*

a) SCAPT3 station, b) SCAPT4 station

the SCAPT1 station is located at a depth of 7.5 m, and the SCAPT4 station is less than 1 m deep. Three stations of SCAPT2, SCAPT3, and SCAPT5 started measuring from 12th to 17th March 2009, while two stations of SCAPT1 and SCAPT4 monitored from 13th March to 22nd April 2009 [22].

Data of currents (magnitude and direction) and waves (significant height) will thus be recorded over a period of one and a half months. However, only the data of SCAPT3 and SCAPT4 located in the seaward and landward directions of the geotube submerged breakwater are used to calibrate and validate in this work.

Concerning SCAPT3, the wave directions are the same as those in SCAPT1 and SCAPT2. Nonetheless, the significant wave heights averaged about 0.2 and 0.4 m during the two periods of bad weather (Figure 4a). The highest wave height in this measurement period reached 0.38 m, corresponding to a wave period of 5.2 s at 11AM on 16th March. There is an asymmetry of waves resulting from waves approaching the coast. The average wave period at this station is approximately 6.2 s.

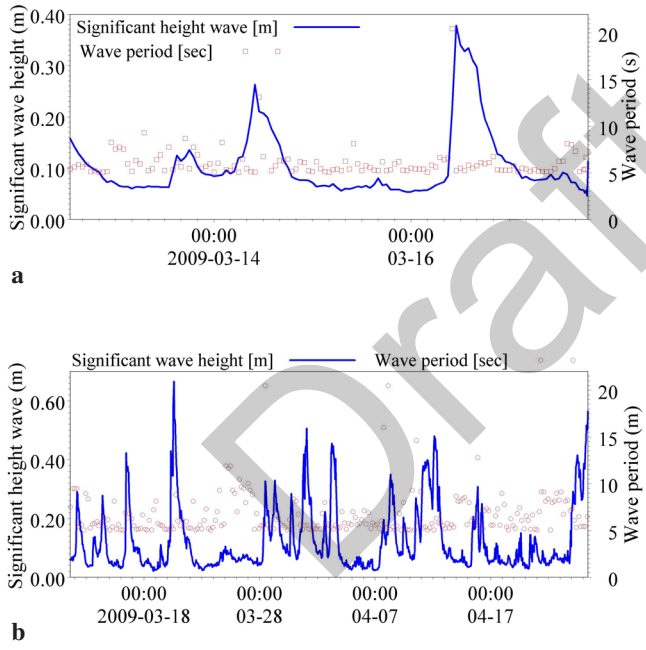

Figure 4. *Measured wave height and wave period at La Capte in 2009 [22]*

a) Current rose, b) Velocity components

The measurement of the wave at the SCAPT4 station located 120 m seaward of the shoreline was carried out in the longest period from 13th March to 22nd April, 2009. The average significant wave height is approximately 0.12 m, but many variations are observed, with the highest wave height of up to 0.67 m. Hence, during this period, the number of waves that exceeded the height threshold of 0.4 m was reached nearly eight times, as depicted in Figure 4b. The wave period at this station varies from 5 to 20 s and averages approximately 6.6 s.

The current data were measured at the SCAPT4 station from 13th March to 22nd April, 2009. During the measurement period, the northern and southern currents were mostly observed, but the northbound currents were still dominant and stronger than those in other directions (Figure 5a). There are two main components of velocities, cross-shore and longshore (Figure 5b). The cross-shore velocities are positive when they are directed shoreward. Conversely, they are negative when they move seaward. It is noted that the currents moving toward the coast are faster than those moving toward the sea, but only extend over a short period. Particularly, from 18th to 28th March 2009, the seaward currents were relatively weak, while the shoreward currents

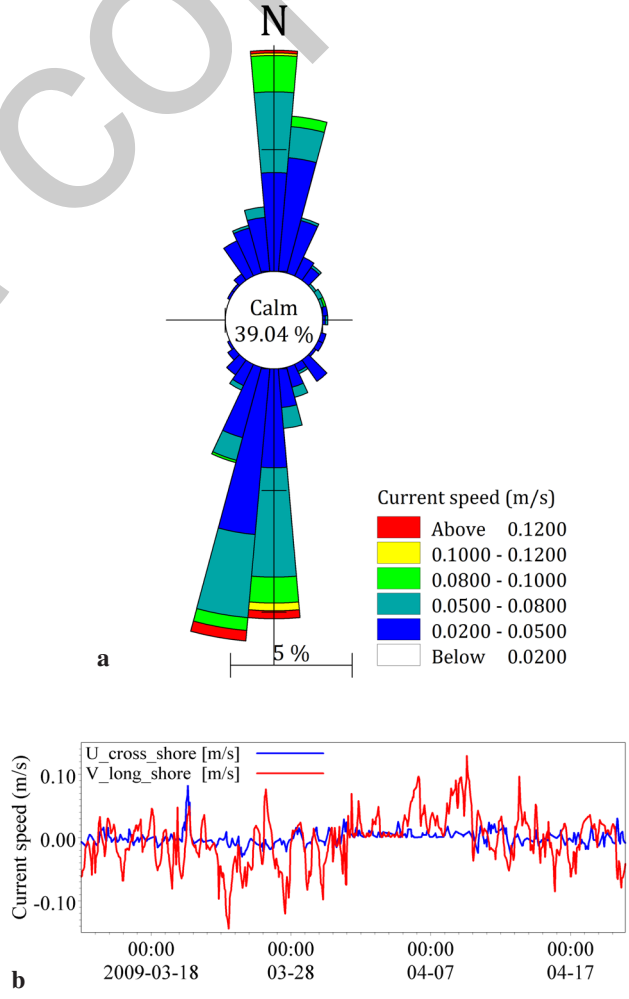

Figure 5. *Nearshore current data from the SCAPT4 station at La Capte beach in 2009 [22]*

a) Wave height, b) Wave period

became stronger between 1st and 4th April, 2009. The main cause of this phenomenon can be attributed to wave action. It is easy to see that the largest cross-shore flow velocities occur at the time of the largest wave heights. In other words, high waves induce cross-shore currents to move shoreward, whereas weak cross-shore currents direct seaward due to small waves. The maximum cross-shore current speed is 0.09 m/s shoreward, whereas the longshore current speed reaches the highest value of 0.14 m/s northward [22].

3.2. Numerical Model Descriptions

The impact of SLR on the hydrodynamics and sediment movement process along the Bona and Ceinturon beaches in the eastern Giens double tombolo was investigated and uncovered using the MIKE21 numerical package [24]. Specifically, the MIKE 21 Spectral Waves (SWs) model is applied to reproduce the swell and wind-induced wave field. The wave-generated currents and water level fluctuation can be simulated in the MIKE 21 Hydrodynamic (HD) model, where the MIKE 21 Sand Transport (ST) model is used to describe the sediment transport and bathymetry change.

The mathematical models will be solved on a computational grid of approximately 30 square kilometers. This grid extends from Salins beach (about 2 km north of the Gapeau river mouth) to La Badine beach (about 9 km south of the Gapeau river mouth). It has three open-sea boundaries in the east, southeast, and south, and a shoreline-land boundary in the west (Figure 2). The southeast open-sea boundary of this domain is 2 km from the coastline. Furthermore, the main flow input, namely the Gapeau river, has also been included in the study domain. The length of this river ends at the Sainte Eulalie station, where no tides are reaching. All these boundaries must be located far enough to ensure that their spurious effect is kept outside the area of interest. The computational grid is built with 13,620 nodes and 22,960 elements. This is also the result of the sensitivity analysis of 15 grids with different resolutions [25]. The smallest grid cell area is approximately 9 m^2 inside the Gapeau river and along the beaches, whereas the largest is approximately 12,000 m^2 in the offshore zone (Figure 2).

3.3. Calibration Parameters

Model calibration is essentially the process of adjusting the governing parameters so that the model can reproduce the physical problem. Nikuradse's roughness height (ks) is used for the SW model to adjust the wave parameters. The distribution of Manning's number (M) in the entire study area is the main factor affecting the water level and current speed in the Hydrodynamic model. In addition, the ST model is calibrated using the median grain size (D_{50}). However, in the study area, the seafloor material is heterogeneous. Specifically, the area near the shore is characterized by sand, whereas the remaining area is covered with Posidonia seagrass interspersed with rocks. Therefore, the parameters of this model calibration will also be determined according to different formulas suitable for each type of seabed material. Details on the calibration procedure of these models are proposed by Vu et al. [20], Liu [26], and Nguyen [27].

This calibration process is performed for periods or events in which the best-fitted observed data are available within the computational domain. In this study, the HD and the SW models are calibrated by the observation data in March and April 2009, whereas the calibration of the ST model is done during the period from November 2007 to November 2008. As recommended by some researchers [26,28-34], the performance evaluation of numerical models is performed using coefficients, including the Root Mean Square error (RMSE), scatter index (SI), and squared multiple correlation coefficient (R^2). In addition, the Brier Skill Score (BSS) is suggested to access the numerical simulation of coastal morphology by Van-Rijn et al. [35], Roelvink et al. [34], Pender and Karunarathna [36].

3.4. Study Scenarios

The input parameters of the simulations that consider the SLR are summarized in Table 1. For normal cases that consider changes in wind direction, the sea level is calculated

Table 1. *Input data of simulation cases for the Ceinturon and Bona beaches*

Case	Sea level (m)	Wind data		Wave data		
		Speed (m/s)	Direction (deg)	$H_{1/3}$ (m)	T_p (s)	MWD (deg)
Annual (A1)	0.5	8.50	60 (NE)	2.18	7.43	115
Annual (A2)		6.48	90 (E)			
Annual (A3)		5.22	120 (SE)			
Decadal storm (S1)	1.30	12.55	90	6.56	9.12	110
Tri-decadal storm (S2)	1.35	19.83	90	7.10	10.3	110
Semi-centennial storm (S3)	1.50	29.59	90	7.34	11	110
Centennial storm (S4)	1.85	36.43	90	7.64	12	110

as the value of the multi-year mean sea level plus (+0.39 m) with the minimum sea level change rate in the Marseille area in the period 2040-2050 (0.11 m) [10]. Meanwhile, the calculated sea level in the storm scenarios is determined by the estimated sea level under these conditions plus the 35 cm increase due to SLR during 2010-2060 [2]. Wind parameters were taken according to the frequency of occurrence from recorded wind data at the Hyères station from 1979 to 2015. The wave parameters used in the simulations were collected from the reports of ERAMM [11] and CEREMA [12].

4. Results and Discussion

In this study, changes in sea level are simulated along with changes in wind direction and stormy variation, thus assessing the impact of these changes on hydrodynamics and sediment dynamics in the area of interest. The values of significant wave height, current speed, sediment transport rate, and bed level change were extracted and compared in a direction perpendicular to the shoreline of Ceinturon and Bona beaches, which are subjected to severe erosion [11]. To quantify the difference between scenarios, these hydrodynamic and sediment transport values at 1.5 m depth at both beaches were also calculated.

4.1. Calibration of the Model

The simulation results of significant wave height and wave period at the SCAPT3 and SCAPT4 stations were extracted and compared with the measurement data. Figures 6 and 7 express the goodness of fit between the field data and the model results. The RMSE ranges between 0.06 and 0.12 m, with a difference between 53% and 98% for wave height at SCAPT3 and SCAPT4 points, respectively. Moreover, the comparison of the wave periods at SCAPT3 and SCAPT4 shows a good fit between the observation and the simulation. The simulation results obtained from the SW model run were then applied across the entire computational domain for the HD model run in March 2009, when the wave radiation varied in time and space. Figure 7c shows a comparison of the observed and simulated current speeds at the SCAPT4 station. It was found to be in good agreement between the observation and simulation. The goodness of fit statistics had an R-square of 0.35, RMSE of 0.03 m/s, and a difference of 90%. In addition, the U and V components of the modeled current velocities are extracted and presented in Figure 8. The trends of the simulated flow velocity components are quite consistent with the results measured by Meulé [22] (Figure 5b). After successfully simulating the real hydrodynamics along the eastern Giens tombolo, the ST model was used to reproduce the sediment dynamics during the 1-year duration (November 2007-2008). The bathymetry of the study area surveyed in 2007 will be used as the input

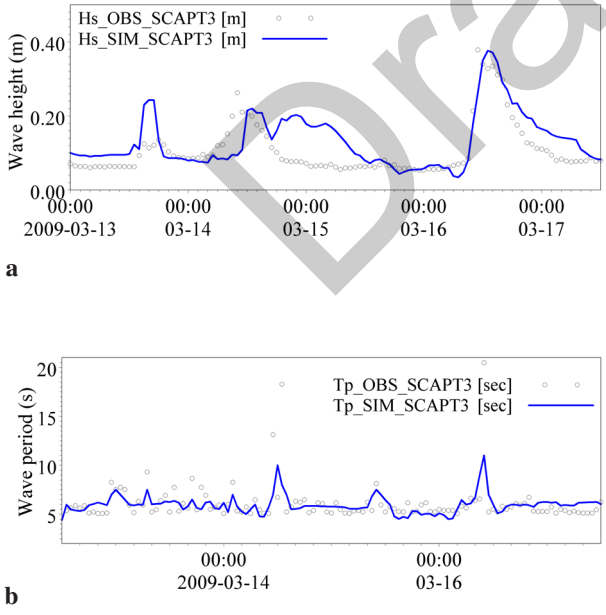

Figure 6. *Time-series plot of the observed (OBS) and simulated (SIM) wave paremeters of the SCAPT3 station*

a) Wave height, b) Wave period

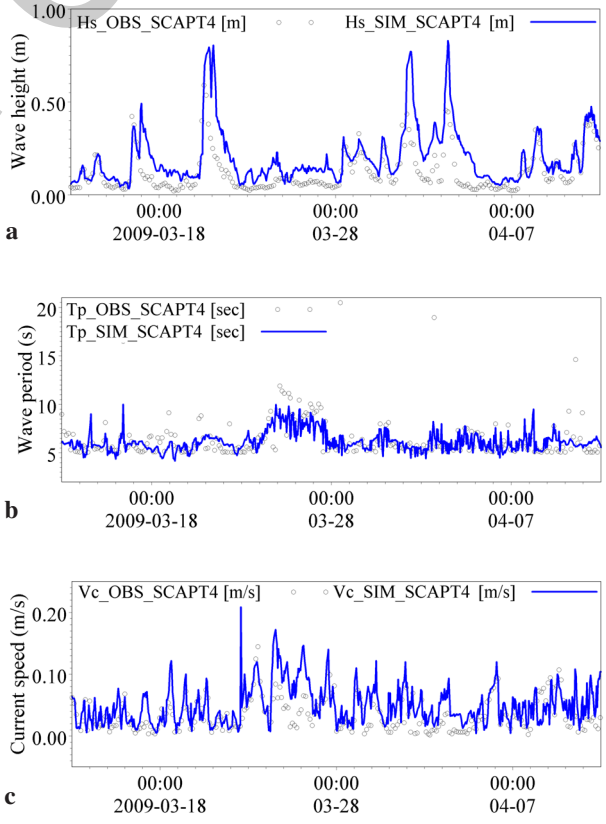

Figure 7. *Time-series plot of the observed (OBS) and simulated (SIM) hydradynamic parameters at the SCAPT4 station*

a) Wave height, b) Wave period, c) Current speed

for this model. A comparison of observed and simulated beach profiles in the south of Ceinturon beach is presented in Figure 9. The statistical error of this comparison (BSS) is found to be 0.61. This confirms that the ST model accurately describes the morphological evolution of the study area [35]. The final set of parameters including Nikuradse roughness height (k_s), Manning's number (M), and median grain size (D_{50}) will be obtained by the calibration processes (Figure 10).

4.2. Impacts of the SLR on Wave Transformation

Due to their geographical location, the beaches located on the eastern branch of the Giens tombolo are directly affected by NE, E, and SW wind-generated waves. In the sea level rise scenario, any change in wind parameters in the three directions mentioned above can cause a large variation in the wave field in the study area. Figure 11a shows the change in wave height in the cross-shore direction under different

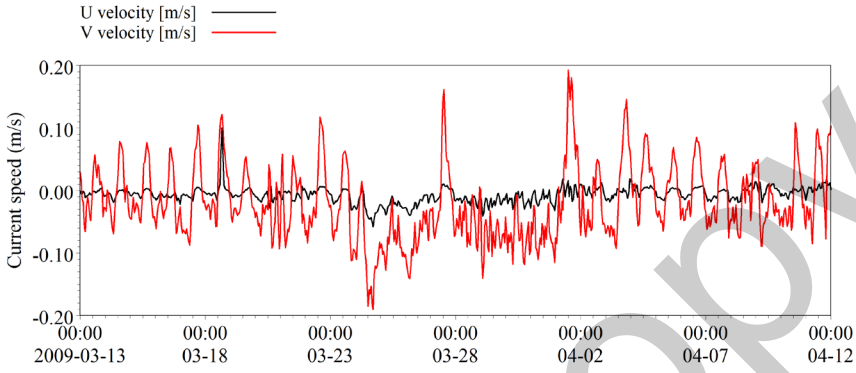

Figure 8. *Time-series plot of the U and V components of the modeled current velocities of the SCAPT4 station*

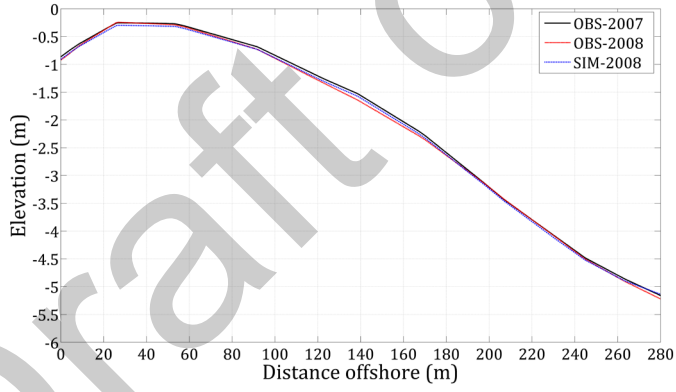

Figure 9. *Comparison of the cross-shore profiles at the Aeroport beach (the south part of the Ceinturon beach)*

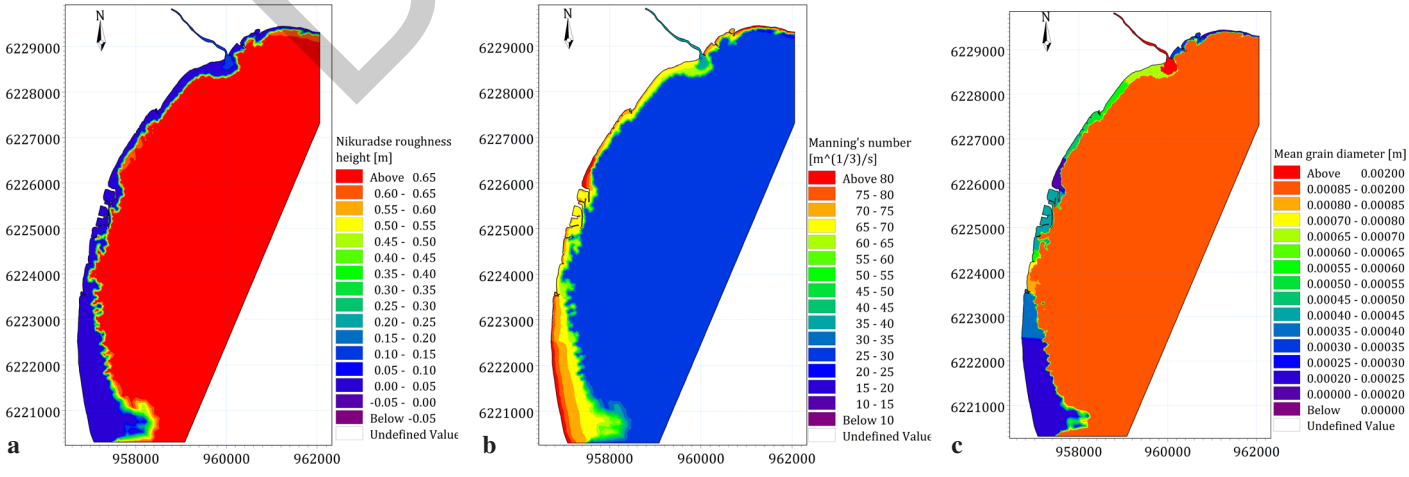

Figure 10. *Spatial distribution of calibration parameters*

a) Nikuradse's roughness height, b) Manning's number, c) Median grain size

wind directions at Bona beach, while the variation in cross-shore wave height at Ceinturon beach in the annual scenarios is presented in Figure 11b. It is noticeable that the highest waves occurring off the coast of Bona beach are induced by the NE waves, where the E winds produce the highest waves off the coast of Ceinturon beach. As these waves approach shallow water, their energy is dissipated by the effect of bottom friction and gradually decreases in height.

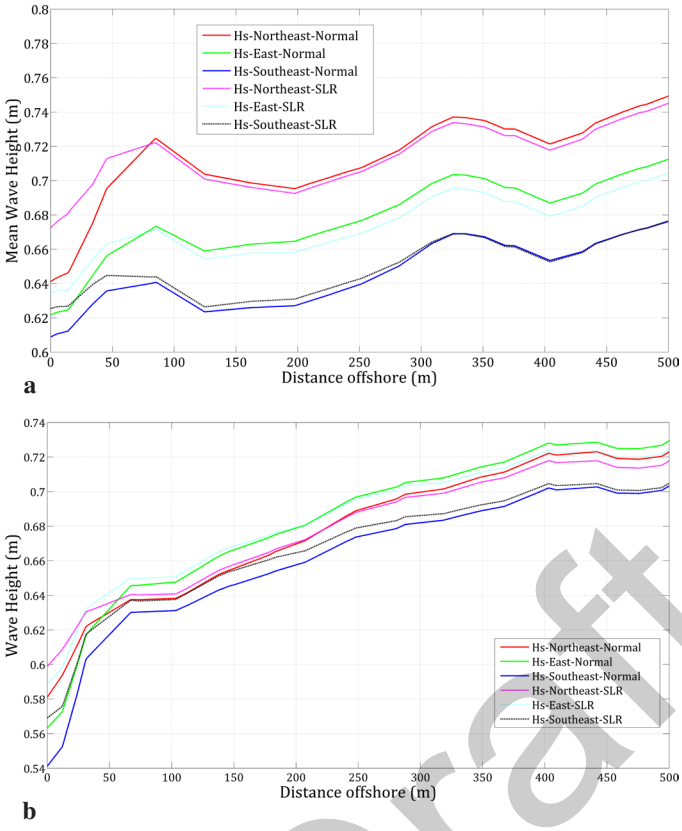

***Figure 11**. Comparison of cross-shore wave heights in different annual cases*

This height reduction differs between the wave directions. In the nearshore area, the NE wind-driven waves are highest at the Bona and Ceinturon beaches. Specifically, the highest significant wave heights appear at the Bona and Ceinturon beaches in the case of northeasterly winds and have values of 0.622 m and 0.682 m, respectively (Table 2). In addition, the results in this table also reveal that the NE winds not only cause the highest waves but also produce the largest radiation stresses (S_{xx}, S_{yy} and S_{xy}). Sea level rise increases the mean wave height in all wind directions at both Ceinturon and Bona beaches by 1.34-2.41% and 1.18-2.86%, respectively. Nevertheless, the magnitude of the increase in wave height is different for each wind direction and beach. Specifically, the NE winds induced the largest increase in wave height of approximately 2.86% at Bona beach, while the largest increase in wave height of approximately 2.41% was found at Ceinturon beach due to the E winds. The main cause of this increase in wave height can be an increase in water depth due to sea level rise, leading to high waves breaking near the shore [37]. Figure 11a illustrates this comment, especially with regard to SE winds. In addition, sea level rise also increases radiation stresses [38]. If SLR is about 11 cm, radiation stresses will increase by about 1-5% for all wind directions at both beaches.

Many extreme events, viz. storms, and rough seas, occur in the winter and attack the Giens tombolo. According to a study conducted by Capanni [19], this is one of the main factors causing coastal erosion on the beaches along the eastern branch of the Giens tombolo. Sea level rise due to climate change and storm surges will facilitate stormy waves that can attack the higher part of the beach and aggravate the problem of coastal erosion in vulnerable beaches [39]. Therefore, the impact of severe storms needs to be investigated in the study area. The change in cross-shore wave heights at the Bona and Ceinturon beaches due to the combined impact of SLR and storms with different frequencies is illustrated in Figure 12.

***Table 2.** Comparison of values of hydrodynamic and sediment dynamics parameters extracted at Ceinturon and Bona beaches under different scenarios*

	Scenario	Ceinturon beach						Bona beach					
		H_s (m)	S_{xx} (m^3/s^2)	S_{xy} (m^3/s^2)	S_{yy} (m^3/s^2)	V_c (m/s)	Q ($m^3/s/m$)	H_s (m)	S_{xx} (m^3/s^2)	S_{xy} (m^3/s^2)	S_{yy} (m^3/s^2)	V_c (m/s)	Q ($m^3/s/m$)
Normal condition	NE	0.622	0.232	-0.064	0.158	0.13	5.05E-05	0.682	0.337	-0.026	0.152	0.103	5.24E-05
	E	0.618	0.228	-0.064	0.155	0.08	3.12E-05	0.649	0.306	-0.028	0.140	0.163	7.35E-05
	SE	0.604	0.216	-0.061	0.147	0.08	3.88E-05	0.631	0.289	-0.029	0.132	0.171	7.57E-05
	Decadal	0.941	0.505	-0.131	0.322	0.16	2.05E-04	1.079	0.803	-0.061	0.352	0.242	4.47E-04
	Tri-decadal	1.027	0.566	-0.149	0.360	0.28	3.73E-04	1.304	1.110	-0.070	0.462	0.205	5.68E-04
	Semi-centennial	1.113	0.648	-0.157	0.380	0.36	6.97E-04	1.393	1.234	-0.050	0.487	0.062	3.99E-04
	Centennial	1.254	0.806	-0.191	0.461	0.37	7.98E-04	1.512	1.412	-0.069	0.563	0.054	4.63E-04

Table 2. *Continued*

	Scenario	Ceinturon beach						Bona beach					
		H_s (m)	S_{xx} (m^3/s^2)	S_{xy} (m^3/s^2)	S_{yy} (m^3/s^2)	V_c (m/s)	Q ($m^3/s/m$)	H_s (m)	S_{xx} (m^3/s^2)	S_{xy} (m^3/s^2)	S_{yy} (m^3/s^2)	V_c (m/s)	Q ($m^3/s/m$)
Sea-level rise	NE	0.631	0.237	-0.065	0.161	0.13	4.93E-05	0.702	0.354	-0.026	0.159	0.081	4.47E-05
	E	0.633	0.237	-0.066	0.161	0.09	3.48E-05	0.656	0.311	-0.028	0.142	0.133	5.79E-05
	SE	0.618	0.227	-0.064	0.155	0.06	2.90E-05	0.641	0.296	-0.029	0.137	0.154	6.60E-05
	Decadal	1.020	0.596	-0.157	0.383	0.13	1.81E-04	1.141	0.923	-0.063	0.389	0.049	1.84E-04
	Tri-decadal	1.142	0.703	-0.180	0.433	0.25	3.54E-04	1.404	1.264	-0.083	0.529	0.184	5.27E-04
	Semi-centennial	1.215	0.766	-0.193	0.461	0.31	5.56E-04	1.487	1.374	-0.066	0.556	0.071	4.59E-04
	Centennial	1.350	0.920	-0.219	0.522	0.33	6.74E-04	1.584	1.531	-0.087	0.620	0.056	5.18E-04
Difference (%)	NE	1.34	2.11	1.88	2.06	2.09	-2.49	2.86	4.97	1.03	4.36	-24.0	-14.63
	E	2.41	4.22	3.38	3.53	4.35	11.35	1.18	1.83	-1.41	1.66	-18.4	-21.15
	SE	2.35	4.83	4.66	4.99	-21.0	-25.13	1.61	2.64	0.21	3.34	-9.87	-12.83
	Decadal	8.36	18.04	19.71	18.93	-22.0	-11.42	5.82	14.96	2.64	10.31	-79.8	-58.89
	Tri-decadal	11.23	24.07	20.3	20.43	-9.16	-5.35	7.65	13.91	19.6	14.5	-10.4	-7.25
	Semi-centennial	9.12	18.19	22.48	21.29	-13.3	-20.35	6.78	11.35	31.05	14.09	15.24	15.2
	Centennial	7.65	14.19	14.49	13.31	-10.9	-15.57	4.8	8.41	25.68	10.23	4.18	11.86

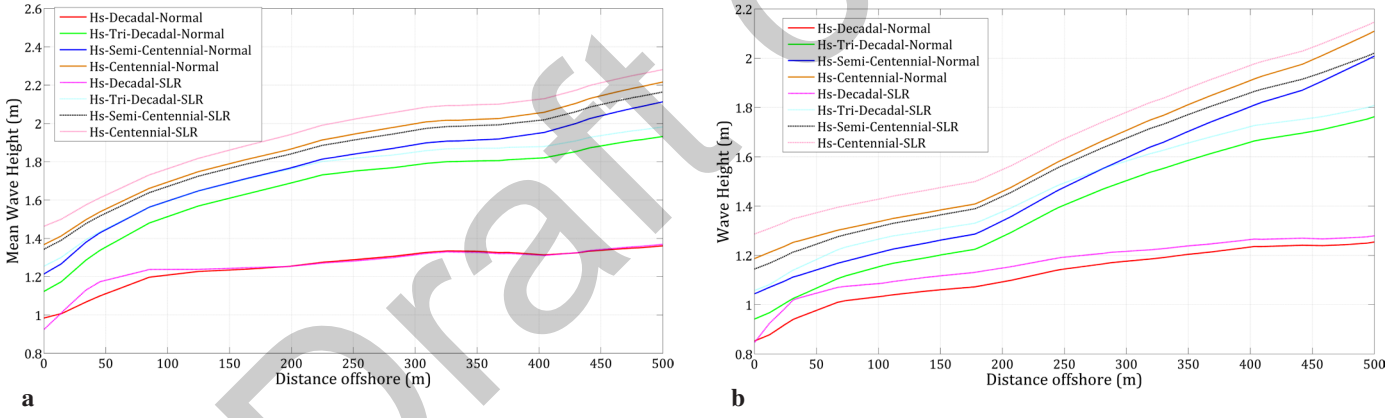

Figure 12*. Comparison of cross-shore wave heights in the different stormy cases*

Obviously, the lower the frequency of the storm, the higher the waves will be generated in both the case with and without sea level rise. Specifically, the significant wave height at Bona beach increased from 1.08 m in a decadal storm to 1.51 m in a centennial storm (Table 2), regardless of sea level rise due to climate change. Meanwhile, the significant wave height at the Ceinturon beach increased from 0.94 m in a decadal storm to 1.25 m in a centennial storm without considering SLR due to climate change. In addition, the simulation results demonstrate that higher waves often attack Bona beach instead of Ceinturon beach during the same storm. The average wave height during storms at Bona beach is greater than that at the Ceinturon beach by about 14.7-27% in conditions without SLR and 11.9-22.9% in conditions of SLR. The cause of this difference may be due to seabed bathymetry. Specifically, the bottom bathymetry at Bona beach is steep and deep, whereas the bottom bathymetry at Ceinturon beach is quite gentle and shallower (Figure 2). Therefore, higher waves can aproach and break closer to Bona beach than to Ceinturon beach. Table 2 also reveals that the nearshore significant wave height is enhanced by about 8.41-14.96% at Bona beach and by about 7.65-11.23% at Ceinturon beach when considering the impact resonance of sea level rise due to climate change and storms. Consequently, the radiation stress will also be increased proportionally to the wave height. Specifically, the radiation stress at the Bona and Ceinturon beaches increased to about 2.64-31.05% and about 13.31-24.07%, respectively, when compared with

scenarios excluding sea level rise due to climate change. This confirms that climate change-induced sea level rise and storm surge increase water depth and reduce wave energy dissipation due to bottom friction, resulting in higher waves reaching the beaches. In the condition of a centennial storm, the radiation stresses increased to relative minima, probably due to the sharp increase in water volume as a result of the submergence of the shore.

4.3. Impacts of the SLR on Current Speed

The simulation results of the cross-shore current speeds generated by different wind directions at the Bona and Ceinturon beaches are shown in Figure 13. It can be easily

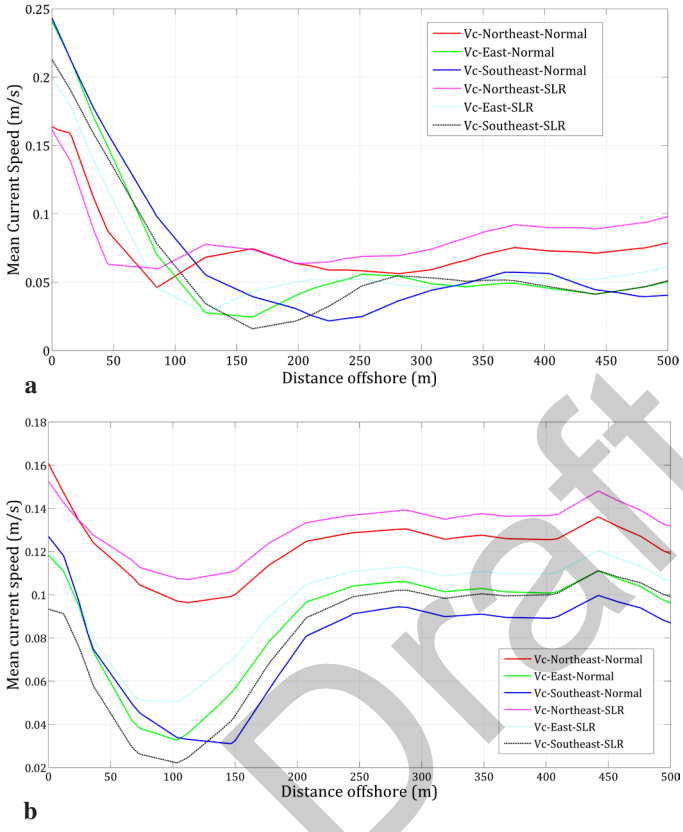

***Figure 13**. Comparison of cross-shore current speeds in the different annual cases*

seen that the offshore current speed in the study area is greatly influenced by the NE winds when sea level rise is not considered. However, the degree of influence of wind directions in the surf zone in the study area changed because of the location of these beaches and the depth of the seabed. Specifically, the NE winds produced the highest mean current speed of 0.128 m/s, approximately 58% higher than other wind directions at the Ceinturon beach. Conversely, the NE winds generate lower currents than the E and SE winds, about 58-66% (Table 2). The breakwaters of the port of Hyères are the main cause of this discrepancy. The longshore currents induced by the NE winds move along the coast from Salins beach to Hyères port, and then they have to change direction and flow seaward after meeting with the breakwaters of Hyères port [18].

As a result, the speed of these currents is reduced much more after reaching Bona beach right downstream of the structures. Meanwhile, the currents generated by the E and SE winds approach this beach without any obstacles. In Bona beach, the highest current speed was induced by SE winds, whereas NE winds generated the largest waves. This proves that wind factors mainly influence nearshore currents. At the same time, waves play only a minor role in the development of these currents. SLR causes offshore currents (from a depth of about 150 m to offshore) to be stronger than those in scenarios excluding sea level rise. In contrast, nearshore currents under normal sea level conditions are higher than those in sea level rise scenarios. Table 2 reveals that the nearshore current speed caused by the SE winds at the Ceinturon beach decreased by 21% if the sea level increased. At Bona beach, the nearshore current speeds in all wind directions are reduced by 9.87-24% compared with the cases excluding sea level rise. The decrease in current speed has been attributed to the local expansion of water volumes due to the SLR and inundation of low-lying beaches. The current speed can decrease from depths 50 m offshore at Ceinturon beach and from depths 100 m offshore at Bona beach in both seasonsThe current speed maintains a reduction trend from a depth of 50 m offshore at Ceinturon beach and from a depth of 100 m offshore at Bona beach in both the normal water level and sea level rise scenarios. Then, the cross-shore currents increase sharply before they reach the shoreline. This increase in current speed in these areas can be attributed to the breaking wave energy [38]. The swift reduction in the current speed at these positions was caused by sand bars and troughs (Figure 2). Incoming waves break when they pass over the sand bars. Subsequently, the presence of troughs causes a decrease in wave-induced radiation stresses due to increased water depth. When the breaking waves approach the shore, accompanied by decreased water depth, the radiation stresses intensify again. This results in a sharp increase in current speed close to the shore.

Figure 14 shows the change in cross-shore current speed at the Bona and Ceinturon beaches under the combined impacts of sea level rise and different storm levels (decadal storm, tricadal storm, semi-centennial storm, and centennial storm). Stronger storms generate higher speed currents at Ceinturon beach. Indeed, the higher the storm level, the greater the wave height. As a result, higher wave heights result in faster current speeds. In particular, the current speed during decadal, tri-decadal, semi-centennial, and centennial storms was recorded as 0.164, 0.276, 0.36, and

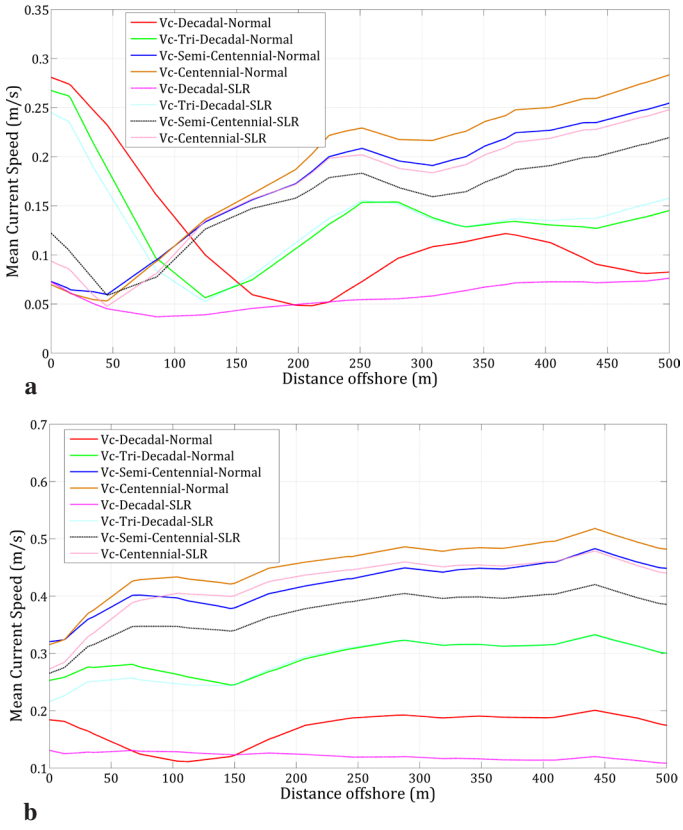

***Figure 14**. Comparison of cross-shore current speeds in the different stormy cases*

0.371 m/s at this beach, respectively. In addition, the current speed at Ceinturon beach is often greater than that at Bona beach during the same storm, regardless of sea level rise. Specifically, the current speed values extracted from Bona beach in the decadal, tri-decadal, semi-centennial, and centennial storm scenarios are 0.242, 0.205, 0.062, and 0.054 m/s, respectively. Similar to the annual scenarios, the main cause of this phenomenon is the appearance of the Hyeres port breakwater, which causes the speed of longshore currents to decrease as they approach Bona beach. At Ceinturon beach, although the current speed is generally reduced, the strong storms still induce high nearshore current speeds (Figure 14b). However, the current field in the surf zone at Bona beach is completely different from that at Ceinturon beach. It is easy to see that the current speeds in all storms are accelerated in the surf zone at the Ceinturon beach (Figure 14a), whereas most of the currents induced by storms occurring at the Bona beach tend to decrease before approaching the shore (Figure 14b). If sea levels rise due to climate change, most of the current speeds during storms are reduced by about 10.4-79.8% at Bona beach and about 9.16-22% at Ceinturon beach. Except for the semi-centiennial and centennial storm scenarios, the current speed near Bona beach increased by 15.24% and 4.18%, respectively (Table 2).

4.4. Impacts of the SLR on Sediment Transport and Beach Morphology

Many researchers [13,15,18,19] have found that the longshore currents generated by the oblique waves approaching the coast govern the law of sediment transport in Hyères Bay. These authors also showed a decrease in sediment grain size in the flow direction from north to south and from east to west. However, the longshore currents and the sediment dynamics field have been modified by cross-shore structures, viz. jetties, breakwaters, and groynes, which were built along the eastern branch of the Giens double tombolo. These structures have caused differences in sediment dynamics between the beaches, especially between Ceinturon beach (upstream of the Hyeres harbor breakwater) and Bona beach (located between the Hyeres harbor breakwaters and the La Capte groyne). The cross-shore changes in sediment transport rates under the dual action of NE, E, and SE winds and sea level rise at the Ceinturon and Bona beaches are shown in Figure 15. It is easy to see that the high sediment transport rates are concentrated mainly between the shoreline and the 150 m offshore location. The main causes of this phenomenon are due to high wave-induced radiation stresses and current speeds (Figure 13). For the area from a depth of 150 m from shore to offshore, the impact of sediment transport is most strongly influenced by the NE winds in both normal and sea

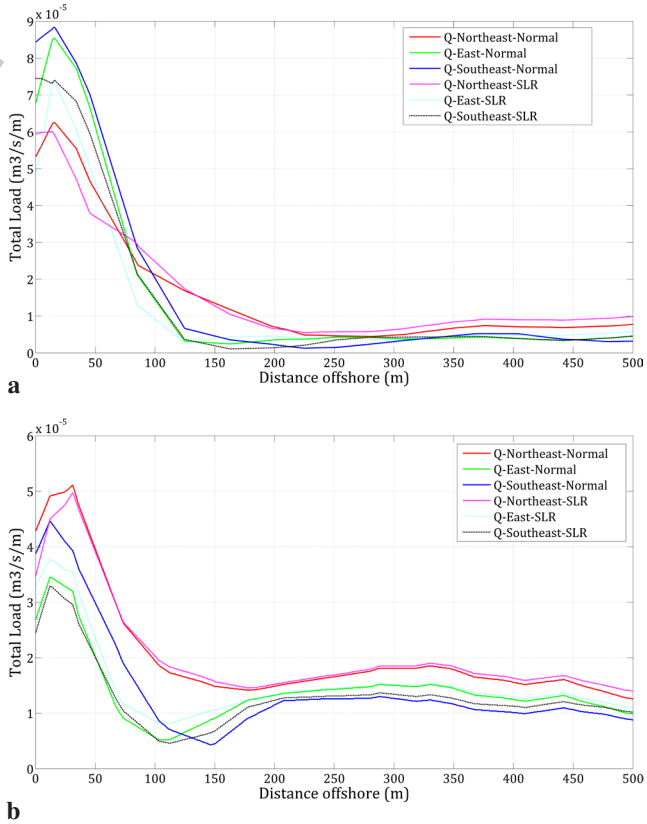

***Figure 15**. Comparison of cross-shore sediment transport rates in the different annual cases*

level rise scenarios. The highest sediment transport rates at Bona and Ceinturon beaches were observed in the NE winds. In addition, northeasterly winds continue to govern the sediment transport in the area from the shoreline to a depth of approximately 150 m offshore at the Ceinturon beach. In addition, in this area, the highest total load of more than $5x10^{-5}$ $m^3/s/m$ was recorded in the NE winds. In contrast, the highest total load of about $9x10^{-5}$ $m^3/s/m$ was triggered by the SE winds at Bona beach. Meanwhile, the NE winds generate the total minimum load in the nearshore area under both normal and sea level rise conditions. The current speed field greatly influences this cross-shore sediment transport distribution (Figure 13). When taking into account the occurrence of sea level rise, the total sediment transport load decreased in the area from the shoreline to a depth of approximately 150 m, but increased significantly in the area from the shoreline depth of 150 m out to offshore at both beaches in all wind directions. Table 2 reveals that the total nearshore sediment transport load is reduced by 12.83-21.15% at Bona beach and 2.49-25.13% at Ceinturon beach, respectively, due to SLR. The main cause may be a decrease in coastal current speed as water depth increases.

Similar to the current and wave fields, the sediment dynamics in the study area are greatly influenced by extreme weather events, especially storms. The extent of the impact of storms is increasing with the appearance of sea level rise due to global climate change. This could be explained by the increased frequency of bigger storms with sea level rise, resulting in larger waves approaching higher beach areas and wave-driven currents moving more sediment volume. Figure 16 illustrates the cross-shore variation of the sediment transport rate at the Bona and Ceinturon beaches due to the impact of stormy scenarios. It is noticeable that high sediment transport rates are observed in the 100-250 m offshore area at Bona beach (Figure 16a). In contrast, high sediment transport rates occur in the coastal area along the shoreline from 50 m to 150 m at Ceinturon beach (Figure 16b) both with and without regard to SLR. In addition, the centennial storm caused the highest sediment transport rates at both beaches (above $1.1x10^{-3}$ $m^3/s/m$). As sea levels rise, most sediment transport rates at the Ceinturon and Bona beaches decrease. Specifically, the sediment transport rate at Ceinturon beach decreased from 5.35% to 20.35% in all storms (Table 2). Meanwhile, the sediment transport rate at Bona beach decreased in the decadal and tri-decadal storm scenarios but increased by about 11.86-15.2% in the semi-centennial and centennial storm conditions. The decrease in sediment transport rates can be mainly attributed to the decrease in current speed as the sea level rises.

The consequence of sea level rise is that the river mouth and estuaries tend to enlarge, and the speed of fluvial currents

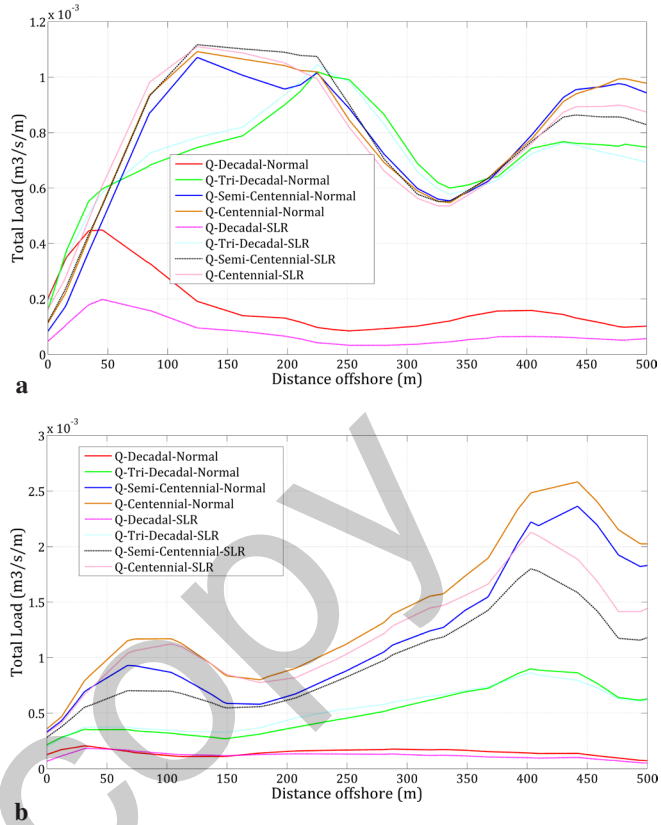

***Figure 16**. Comparison of cross-shore sediment transport rates in the different stormy cases*

will also be reduced by further intrusion of sea currents into the inland; the sediment is deposited right in the river mouth and estuaries [40]. This leads to a shortage of sediment in the downstream zones. The dual effect of this low sediment supply rate and rapid sea level rise is likely to increase the risk of shoreline erosion. To illustrate the change in beach bathymetry under the influence of sea level rise and change in wind direction, beach profiles at Ceinturon and Bona beaches are extracted and are shown in Figure 17. The change in bed level is usually observed at a distance from the shoreline to a depth of -2.5 m at the Ceinturon beach and from the shoreline to a depth of -5.0 m at the Bona beach in both normal and sea level rise scenarios. In addition, northeast winds caused the largest beach profile change in both Ceinturon and Bona beaches. When the sea level rises, the nearshore beach profile is eroded deeper than in normal sea-level cases. This may be due to the impact of the higher waves and higher radiation stresses generating stronger cross-shore currents, which extract sediment and are suspended by the waves and carried offshore.

The dual impact of storms and SLR will intensify the problem of coastal erosion occurring on the Ceinturon and Bona beaches. The beach profile variation of the Ceinturon beach mainly occurs in the distance from the shoreline to offshore, approximately 150 m (Figure 18a). Meanwhile, the

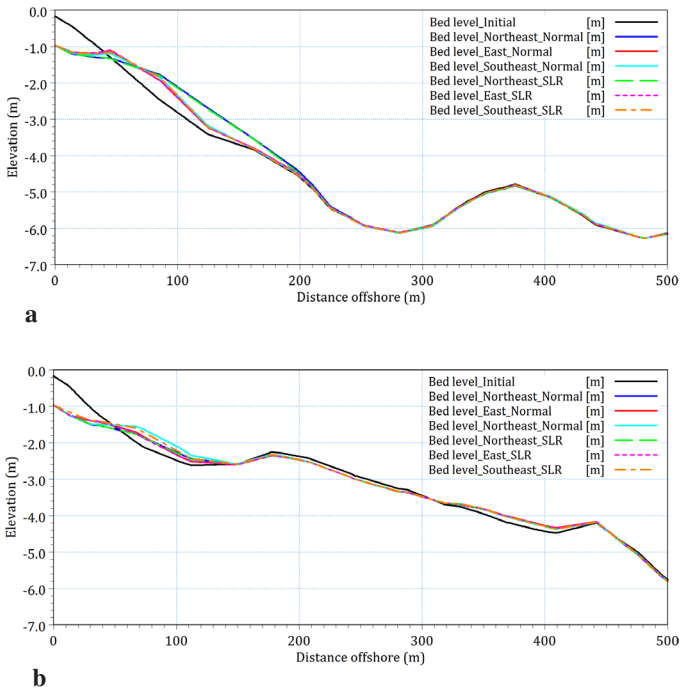

Figure 17. Comparison of beach profile changes in the different annual cases

beach profile variation of Bona beach is mainly concentrated in the distance from the shoreline to offshore, about 330 m (Figure 18b) in both cases, with and without considering SLR. The storms induce high waves, which extract sediment near the shoreline and carry them offshore. The presence of SLR provokes coastal erosion more severely than that

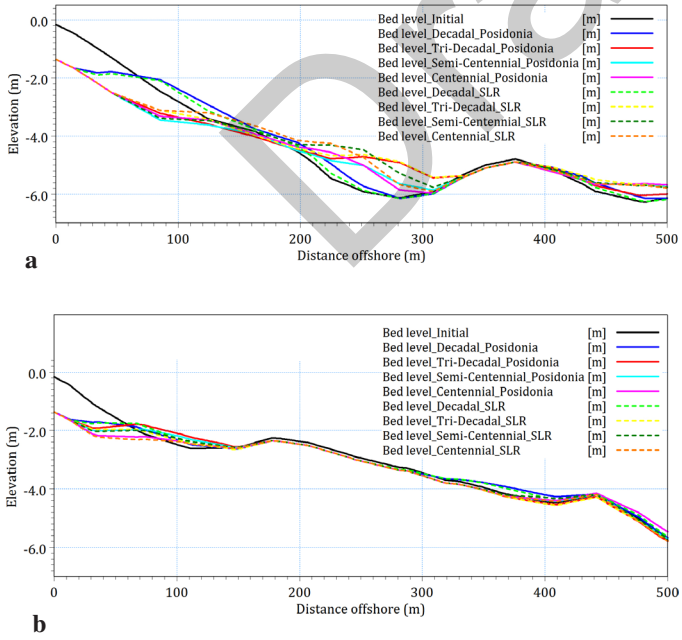

Figure 18. Comparison of beach profile changes in the different stormy cases

in the no SLR scenarios, especially in nearshore zones on both beaches. The comparison of beach profile changes also demonstrates that the severity of coastal erosion depends on the storm level.

Additionally, the erosive mode at Bona beach is more severe than that at Ceinturon beach. The eroded area extends from the shoreline to a depth of 4.5 m offshore at Bona beach. The main reason may be that its location is exposed to storm waves, so higher waves can easily reach this beach. At the same water depth of 1.5 m, the wave heights observed at Bona beach are larger than those at Ceinturon, about 14.67-26.97% without sea-level rise and about 11.86-22.94% with SLR (Table 2).

5. Conclusion

The influence of the SLR on the hydrodynamic field around the Ceinturon and Bona beaches in the eastern Giens double tombolo has been successfully quantified using numerical models. The numerical simulation results confirmed that the presence of SLR could increase wave height but decrease current speed in the surf zone. The increase in wave height under storm conditions is much larger than that under annual conditions. In addition, under annual conditions, NE winds have the greatest influence on wave height in the study area. Under stormy conditions, significant wave heights near shore increased from 7.65% to 11.23% in Ceinturon beach and from 8.41% to 14.96% in Bona beach under stormy conditions. Simultaneously, it only increased by about 1.34-2.41% in Ceinturon beach and 1.18-2.86% in Bona beach in annual scenarios due to SLR. By contrast, a decrease in current speed of about 9.87-24% and 9.16-79.8% is observed at both beaches in the annual and stormy scenarios, respectively, in the case of SLR. The decrease in current speed is attributed as the main cause of the 2.49-25.13% reduction in sediment transport rate, regardless of wave conditions. Although the total load and the mean current speed reduce when the sea level rises, the beach erosion rate is higher than without a rise in the sea level.

With the above-mentioned conclusions, sea level rise due to climate change has a very significant impact on the hydrodynamic mechanism and sediment transport along the Ceinturon and Bona beaches. This makes the erosion of these beaches more serious. Therefore, solutions to adapt to sea level rise and limit the impact of this phenomenon on beach stability need to be considered in future studies.

Acknowledgements

The authors would like to express their sincere gratitude to the Ministry of Education and Training, Vietnam (grant no.: 911) for financial support. The authors are equally thankful to Mr. Samuel Meule, OL, CETMEF, CEREMA, SHOM, and REFMAR for sharing the measured data and to DHI for generously providing MIKE software for research purposes.

Authorship Contributions

Concept design: M. T. Vu, and Y. Lacroix, Data Collection or Processing: M. T. Vu, and Y. Lacroix, Analysis or Interpretation: M. T. Vu, and V. T. Nguyen, Literature Review: M. T. Vu, Y. Lacroix, and V. T. Nguyen, Writing, Reviewing and Editing: M. T. Vu, and V. T. Nguyen.

Funding: Financial support was received from the Ministry of Education and Training, Vietnam (grant no.: 911).

References

[1] IPCC, "The Physical Science Basis", 2021.

[2] M. Tsimplis, M. Marcos, S. Somot, and B. Barnier, "Sea level forcing in the Mediterranean Sea between 1960 and 2000". *Global and Planetary Change,* vol. 63, pp. 325-332, Nov 2008.

[3] D. Gomis, et al. "Sea level rise and its forcing in the Mediterranean Sea". *MedCLIVAR – Mediterranean CLImate VARiability,* 2011.

[4] A. Cazenave, C. Cabanes, K. Dominh, M. C. Gennero, and C. Provost, "Present-day sea level change: observations and causes". in *Earth Gravity Field from Space — From Sensors to Earth Sciences: Proceedings of an ISSI Workshop 11–15 March 2002, Bern, Switzerland*, G. Beutler, M. R. Drinkwater, R. Rummel, and R. Steiger, Eds. Dordrecht: Springer Netherlands, 2003, pp. 131-144.

[5] G. Galassi, and G. Spada, "Sea-level rise in the Mediterranean Sea by 2050: Roles of terrestrial ice melt, steric effects and glacial isostatic adjustment". *Global and Planetary Change,* vol. 123, Part A, pp. 55-66, Dec 2014.

[6] R. P. Paskoff, "Effects of sea-level rise on coastal cities and residential areas". In *Climate Change, Human Systems and Policy*. vol. 2, A. Yotova, Ed., ed: Eolss Publishers Co. Ltd.,, 2009, pp. 1-16.

[7] P. Vellinga and S. P. Leatherman, "Sea level rise, consequences and policies". *Climatic Change,* vol. 15, pp. 175-189, 1989.

[8] N. R. Council, D. E. L. Studies, O. S. Board, B. E. S. Resources, and O. W. Committee on Sea Level Rise in California, *Sea-Level Rise for the Coasts of California, Oregon, and Washington: Past, Present, and Future*: National Academies Press, 2012.

[9] R. Ranasinghe, "Assessing climate change impacts on open sandy coasts: A review". *Earth-Science Reviews,* vol. 160, pp. 320-332, Sep 2016.

[10] C. Brunel, and F. Sabatier, "Potential influence of sea-level rise in controlling shoreline position on the French Mediterranean Coast". *Geomorphology,* vol. 107, pp. 47-57, Jun 2009.

[11] V. M. Tuan, Y. Lacroix, and V. Q. Hung, "Assessment of the Shoreline Evolution at the Eastern Giens Tombolo of France". In *Proceedings of the International Conference on Innovations for Sustainable and Responsible Mining*, Cham, 2021, pp. 349-372.

[12] J. J. Blanc, «Phénomènes d'érosions sous-marines à la Presqu'île de Giens (Var),» *CR Acad. Sci. Paris,* vol. 278, pp. 1821-1823, 1974.

[13] A. J. D. Grissac, "Dynamic sedimentology of the Hyères and Giens bays (Var). Planning problems," Ph.D. dissertation, University of Aix-Marseille II, Marseille, 1975.

[14] Y. Lacroix, M. T. Vu, V. V. Than, and V. T. Nguyen, "Modeling the effect of geotextile submerged breakwater on hydrodynamics in La Capte beach". In *Vietnam-Japan Workshop on Estuaries, Coasts and Rivers*, Hoi An, Vietnam, 2015.

[15] M. T. Vu, Y. Lacroix, and V. T. Nguyen, "Empirical equilibrium beach profiles along the Eastern Tombolo of Giens". *Journal of Marine Science and Application,* vol. 17, pp. 241-253, Jun 2018.

[16] M. T. Vu, Y. Lacroix, and V. T. Nguyen, "Investigating the effects of sea-level rise on morphodynamics in the western Giens tombolo, France". *IOP Conference Series: Earth and Environmental Science,* vol. 167, 012027, Jul 2018.

[17] J. J. Blanc, "Recherches sédimentologiques sur la protection du littoral à la presqu'ile de Giens (Var)". Rapport final 1973.

[18] J. Courtaud, "Geomorphological dynamics and coastal risks case of the tombolo of Giens (Var, southern France)". Ph.D. dissertation, University of Aix-Marseille I, 2000.

[19] R. Capanni, "Study and integrated management of sediment transport in the Gapeau river/ Hyères bay system". Ph.D., University of Aix Marseille 1, 2011.

[20] M. T. Vu, Y. Lacroix, and V. T. Nguyen, "Investigating the impacts of the regression of Posidonia oceanica on hydrodynamics and sediment transport in Giens Gulf". *Ocean Engineering,* vol. 146, pp. 70-86, Jan 2017.

[21] J. M. Sinnassamy, and C. Pergent-Martini, "Localisation et état de l'herbier de Posidonies sur le littoral P.A.C.A: Var". D.R.A.E. & G.I.S. Posidonie 1990.

[22] S. Meulé, «IMplantation d'Atténuateur de Houle en GEOtextile: Suivi scientifique de la plage de La Capte, Hyères, Var : Instrumentation, Modélisation,» Hyères, Rapport final2010.

[23] E.O.L, "Monitoring of the evolution of the beaches of the commune of Hyères-les-palmiers," Municipality of Heres-Les-Palmiers, Rapport final 2010.

[24] DHI, "MIKE 21 & MIKE 3 FLOW MODEL FM - Hydrodynamic and Transport Module - Scientific Documentation," 2014.

[25] M. T. Vu, "A numerical Approach for the design of coastal protection works in the oriental Tombolo of the Giens Peninsula," Université de Toulon, 2018.

[26] Z. Liu, "Hydrodynamic and Sediment Transport Numerical Modelling and Applications at Tairua Estuary, New Zealand" Doctor of Philosophy, University of Waikato, 2014.

[27] V. T. Nguyen, "Morphological evolution and back siltation of navigation channel in Dinh An Estuary, Mekong River Delta: understanding, simulating and soluting," Doctor of Philosophy, Hohai University, 2012.

[28] M. Hsu, A. Kuo, J. Kuo, and W. Liu, "Procedure to calibrate and verify numerical models of estuarine hydrodynamics". *Journal of Hydraulic Engineering,* vol. 125, pp. 166-182, Feb 1999.

[29] W. Liu, M. Hsu, and A. Kuo, "Modelling of hydrodynamics and cohesive sediment transport in Tanshui River estuarine system, Taiwan". *Marine Pollution Bulletin,* vol. 44, pp. 1076-1088, Oct 2002.

[30] H. S. Mashriqui, "Hydrodynamic and Sediment Transport Modeling of Deltaic sediment processes," Doctor of Philosophy, Department of Civil and Environmental Engineering, Louisiana State University, 2003.

[31] J. Sutherland, A. H. Peet, and R. L.Soulsby, "Evaluating the performance of morphological models". *Coastal Engineering,* vol. 51, pp. 917-939, 2004.

[32] J. Sutherland, D. J. R. Walstra, T. J. Chesher, L. C. van Rijn, and H. N. Southgate, "Evaluation of coastal area modelling systems at an estuary mouth". *Coastal Engineering,* vol. 51, pp. 119-142, 2004.

[33] C. Brière, S. Abadie, P. Bretel, and P. Lang, “Assessment of TELEMAC system performances, a hydrodynamic case study of Anglet, France,” *Coastal Engineering,* vol. 54, pp. 345-356, 2007.

[34] D. Roelvink, A. Reniers, A. van Dongeren, J. van Thiel de Vries, R. McCall, and J. Lescinski, “Modelling storm impacts on beaches, dunes and barrier islands". *Coastal Engineering,* vol. 56, pp. 1133-1152, Nov-Dec 2009.

[35] L. C. Van-Rijn, D. J. R. Walstra, B. Grasmeijer, J. Sutherland, S. Pan, and J. P. Sierra, “The predictability of cross-shore bed evolution of sandy beaches at the time scale of storms and seasons using process-based profile models". *Coastal Engineering,* vol. 47, pp. 295-327, 2003.

[36] D. Pender, and H. Karunarathna, “A statistical-process based approach for modelling beach profile variability”. *Coastal Engineering,* vol. 81, pp. 19-29, Nov 2013.

[37] C. D. Storlazzi, E. Elias, M. E. Field, and M. K. Presto, “Numerical modeling of the impact of sea-level rise on fringing coral reef hydrodynamics and sediment transport". *Coral Reefs,* vol. 30, pp. 83-96, 2011.

[38] S. K. Liu, “Using coastal models to estimate effects of sea level rise". *Ocean & Coastal Management,* vol. 37, pp. 85-94, 1997.

[39] R. J. N. Devoy, “Coastal Vulnerability and the Implications of Sea-Level Rise for Ireland". *Journal of Coastal Research,* vol. 24, pp. 325-443, 2008.

[40] P. D. Komar, *Beach Processes and Sedimentation*: Prentice Hall, 1998.